

Fluorowardite, $\text{NaAl}_3(\text{PO}_4)_2(\text{OH})_2\text{F}_2 \cdot 2\text{H}_2\text{O}$, the fluorine analog of wardite from the Silver Coin mine, Valmy, Nevada

ANTHONY R. KAMPF^{1,*}, PAUL M. ADAMS², ROBERT M. HOUSLEY³ AND GEORGE R. ROSSMAN³

¹Mineral Sciences Department, Natural History Museum of Los Angeles County, 900 Exposition Boulevard, Los Angeles, California 90007, U.S.A.

²126 South Helberta Avenue, #2, Redondo Beach, California 90277, U.S.A.

³Division of Geological and Planetary Sciences, California Institute of Technology, Pasadena, California 91125, U.S.A.

ABSTRACT

Fluorowardite (IMA2012-016), $\text{NaAl}_3(\text{PO}_4)_2(\text{OH})_2\text{F}_2 \cdot 2\text{H}_2\text{O}$, the F analog of wardite, is a new mineral from the Silver Coin mine, Valmy, Iron Point district, Humboldt County, Nevada, U.S.A., where it occurs as a low-temperature secondary mineral in complex phosphate assemblages rich in Al, Na, and F. Fluorowardite forms colorless to white or cream-colored, tetragonal-pyramidal crystals up to 0.1 mm in diameter. The streak is white. Crystals are transparent to translucent, with vitreous to pearly luster. The Mohs hardness is about 5, the tenacity is brittle, the fracture is irregular, and crystals exhibit one perfect cleavage on {001}. The calculated density is 2.760 g/cm³. Optically, fluorowardite is uniaxial positive, with $\omega = 1.576(2)$ and $\epsilon = 1.584(2)$ (white light) and is non-pleochroic. Electron microprobe analyses (average of 8) provided: Na₂O 6.27, CaO 1.74, MgO 0.42, Al₂O₃ 35.21, Fe₂O₃ 0.72, P₂O₅ 32.49, As₂O₅ 0.64, F 6.76, O=F -2.85, H₂O 13.35 (structure), total 94.74 wt%. The presence of H₂O and OH and the absence of CO₃ were confirmed by FTIR spectroscopy. The empirical formula (based on 14 anions) is: $(\text{Na}_{0.87}\text{Ca}_{0.13}\text{Mg}_{0.04})_{\Sigma 1.04}(\text{Al}_{2.96}\text{Fe}_{0.04}^{3+})_{\Sigma 3.00}(\text{P}_{1.96}\text{As}_{0.03})_{\Sigma 1.99}\text{O}_{8.12}(\text{OH})_{2.35}\text{F}_{1.53} \cdot 2\text{H}_2\text{O}$. Fluorowardite is tetragonal, $P4_12_1$, $a = 7.077(2)$, $c = 19.227(3)$ Å, $V = 962.8(5)$ Å³, and $Z = 4$. The eight strongest lines in the X-ray powder diffraction pattern are [d_{obs} in Å(I)(hkl)]: 4.766(100)(004,103); 3.099(75)(211,203); 3.008(62)(115,212); 2.834(28)(204,213); 2.597(56)(205); 1.7628(32)(400,401); 1.6592(29) (multiple); and 1.5228(49)(423, 2·2·10). The structure of fluorowardite ($R_1 = 3.15\%$ for 435 $F_o > 4\sigma F$) contains layers parallel to {001} consisting of $\text{Al}\phi_6$ ($\phi = \text{F}, \text{O}, \text{OH}$ or H_2O) octahedra, PO_4 tetrahedra, and $\text{NaO}_6(\text{H}_2\text{O})_2$ polyhedra. The two independent $\text{Al}\phi_6$ octahedra link by corner-sharing to form a square array. Each PO_4 tetrahedron shares corners with three adjacent octahedra in the same square array and a fourth corner with an octahedron in the next layer. The Na atoms reside in the “cavities” in the square array, forming bonds only to O atoms in the same layer. Of the two nearly identical OH sites in the wardite structure, only one is occupied by F in the fluorowardite structure. This is an interesting example of a structure in which OH and F are selectively incorporated into two different, but similar, sites as the result of rather subtle hydrogen bonding influences.

Keywords: Fluorowardite; new mineral; crystal structure; hydrogen bonding; FTIR spectroscopy; Raman spectroscopy; electron microprobe analysis; Silver Coin mine, Valmy, Nevada

INTRODUCTION

Wardite, $\text{NaAl}_3(\text{PO}_4)_2(\text{OH})_4 \cdot 2\text{H}_2\text{O}$, was first described by Davison (1896) from cavities in variscite nodules from Utah. Although not specifically mentioned in that paper, the type locality is the well-known Clay Canyon deposit near Fairfield in Utah County, which is also the type locality for englishite, gordonite, millisite, montgomeryite, and overite. Since that time, wardite has been reported from many other localities worldwide, but has previously not been reported to contain significant amounts of F. The structure of wardite was solved by Fanfani et al. (1970) using a crystal from the type locality. They reported the structure to include two distinct OH sites.

The recognition of wardite crystals in an F-rich secondary

phosphate assemblage at the Silver Coin mine near Valmy, Nevada, led us to extensively survey wardite crystals for high F contents that could correspond to the F analog. We found F to be present in most of the wardite crystals in this assemblage, with contents reaching levels sufficient to take the place of nearly half of the OH in the structure. The refinement of the structure of one of these crystals (see below) showed the F to selectively occupy one of the OH sites, where it is strongly dominant over OH. While it is not entirely clear whether it is possible for both OH sites to be dominated by F, its dominance at one of the sites is sufficient to qualify the phase as a new mineral and the F analog of wardite.

The name is based upon the mineral being the F analog of wardite. Note that “fluoro-” rather than “fluo-” is used as the prefix to make pronunciation more straightforward. The new mineral and name have been approved by the Commission on

* E-mail: akampf@nhm.org

New Minerals, Nomenclature and Classification of the International Mineralogical Association (IMA2012-016). Two co-type specimens are housed in the collections of the Mineral Sciences Department, Natural History Museum of Los Angeles County, catalog numbers 57659 and 63810. Specimen 57659 is also a co-type for meurigite-Na (Kampf et al. 2009).

OCCURRENCE AND PARAGENESIS

Fluorowardite occurs in the phosphate stope at the Silver Coin mine, Valmy, Iron Point district, Humboldt County, Nevada, U.S.A. (40°55'44"N 117°19'26"W). It occurs in association with alunite, barite, cacoxenite, chlorargyrite, fluorapatite, goethite, gorceixite (F-rich), iangreyite, iodargyrite, jarosite, kidwellite, kintoreite/plumbogummite, krásnoite, leucophosphate, lipscombite/zinlipscombite, meurigite-Na, metavariscite, millisite (F-rich), morinite, quartz, rockbridgeite, strengite/variscite, and turquoise/chalcosiderite (minerals separated by slashes exhibit variations in chemistry between the two species). A partial list of mineral species occurring at the Silver Coin mine is given by Thomssen and Wise (2004). The Silver Coin mine is the type locality for zinlipscombite (Chukanov et al. 2006), meurigite-Na (Kampf et al. 2009), iangreyite (Mills et al. 2011), and krásnoite (Mills et al. 2012). Fluorowardite is a low-temperature secondary mineral in complex phosphate assemblages rich in aluminum, sodium, and fluorine.

PHYSICAL AND OPTICAL PROPERTIES

Fluorowardite occurs as colorless to white or cream-colored, tetragonal-pyramidal crystals truncated by the basal pinacoid. The forms observed are {001} (prominent and lustrous), {011} and/or {012} (prominent, irregular, and striated parallel to [100]), and {100} (common, irregular, and striated parallel to [100]). A variety of other minor forms, e.g., {114}, are observed on SEM images, but are uncommon (Figs. 1–3). No twinning was observed. Crystals occur as isolated individuals up to 0.1 mm in diameter and as drusy aggregates.

The streak is white. Crystals are transparent to translucent with vitreous to pearly luster. Fluorowardite does not fluoresce

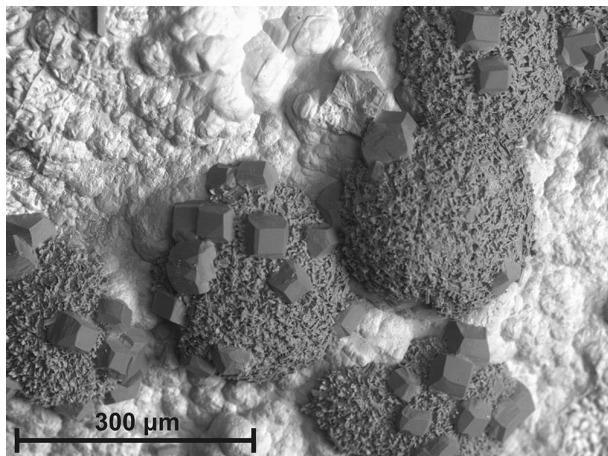


FIGURE 1. Backscatter SEM image of fluorowardite crystals growing on balls of turquoise over lipscombite. The underlying material (white) is goethite.

in long- or short-wave ultraviolet light. The Mohs hardness is about 5, the tenacity is brittle, the fracture is irregular, and crystals exhibit one perfect cleavage on {001}. Attempts to measure the density by sink-float failed because of the small size of the crystals and their near invisibility in available liquids. The calculated density based on the empirical formula and the unit cell refined from the single-crystal data is 2.760 g/cm³. Fluorowardite is unreactive and insoluble in concentrated HCl, concentrated H₂SO₄, and 70% HNO₃, observed over the course of several hours. Optically, fluorowardite is uniaxial positive, with $\omega = 1.576(2)$ and $\epsilon = 1.584(2)$, measured in white light. The mineral is non-pleochroic.

Infrared spectroscopy

An FTIR spectrum (Fig. 4) was obtained with a Thermo-Nicolet Model 6700 spectrometer equipped with a Continuum microscope. A small amount of material was crushed in a

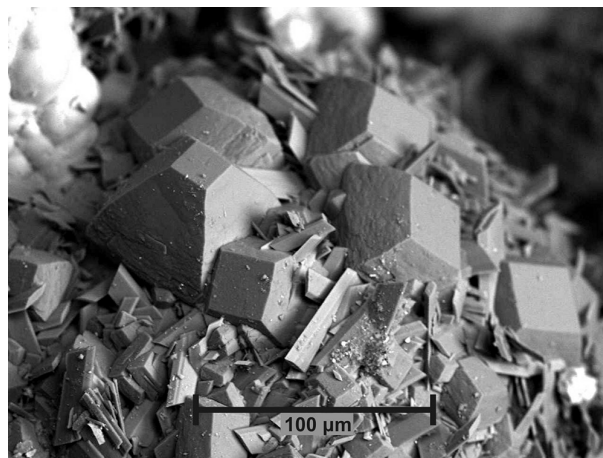


FIGURE 2. Backscatter SEM image of fluorowardite and turquoise crystals.

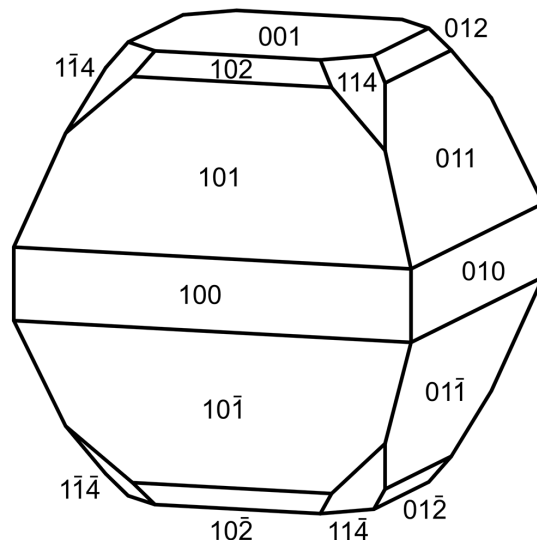


FIGURE 3. Crystal drawing of fluorowardite (clinographic projection).

diamond compression cell and analyzed in transmission through one diamond window. Band assignments are according to Breiter et al. (2004). The main observed bands (in wavenumbers) are: 3615 and 3544 (OH stretching), 3274 and 3153 (H₂O stretching), 1659 (H₂O bending), 1162 and 1131 [δ Al₂(OH)], 1080 (PO₄ antisymmetric stretching), and 1008 (PO₄ symmetric stretching).

Raman spectroscopy

Raman spectroscopic micro-analyses were carried out using a Renishaw M1000 micro-Raman spectrometer system. Light from a 514.5 nm argon laser was focused onto the sample with a 100 \times objective lens, and at 100% power could provide approximately 5 mW of power at the sample, in a spot size of about 1 μ m. Spectral peak positions were periodically calibrated against a silicon standard and rarely varied more than 1 cm⁻¹. All spectra were obtained with a dual-wedge polarization scrambler inserted directly above the objective lens to minimize the effects of polarization.

As a reference for the fluorowardite, we first obtained Raman spectra along the *a*- and *c*-axes of a Rapid Creek, Yukon Territory, Canada, wardite crystal from the Caltech collection (CIT-15080). In these spectra (Figs. 5 and 6), we noted two strong, sharp lines at 3544 and 3616 cm⁻¹ in the OH stretching region. In their recent spectroscopic study of wardite, Frost and Xi (2012) noted similar strong lines in their IR spectra,

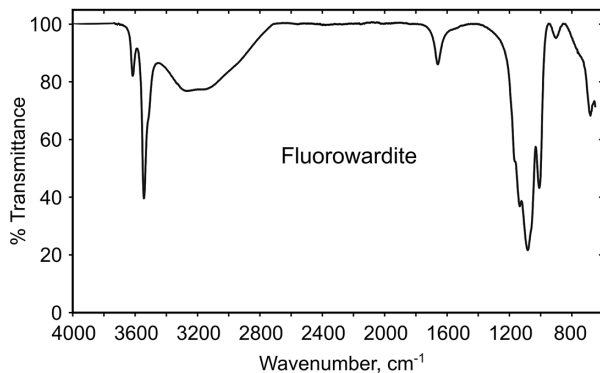


FIGURE 4. FTIR spectrum of fluorowardite.

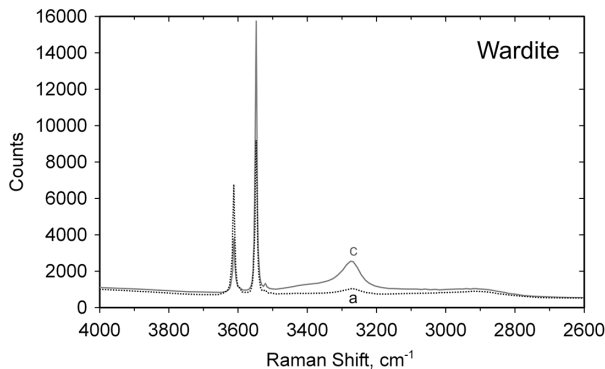


FIGURE 5. Raman spectrum of wardite in the OH region taken with the laser illumination down the *a*- and *c*-axes.

and assigned them to the two crystallographically distinct OH sites in the structure. The difference in vibrational energy in these two otherwise similar sites already supports the view that they might have significantly different preferences for OH, in agreement with the conclusions of the X-ray study.

For the fluorowardite, spectra were first collected from crystals in the microprobe section. These consisted of an arc of crystals individually about 40 μ m across surrounding a hemisphere of material of undetermined composition, mounted in

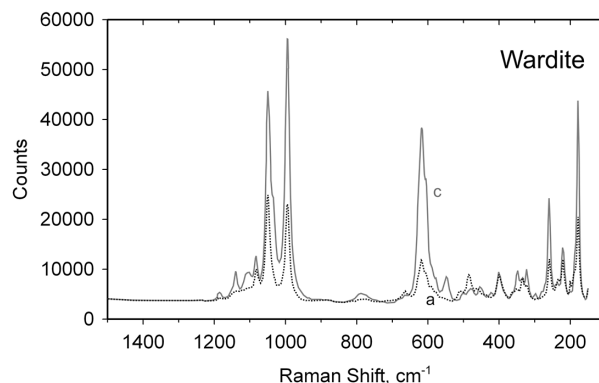


FIGURE 6. Raman spectrum of wardite in the lower wavenumber region obtained with the laser illumination down the *a*- and *c*-axes.

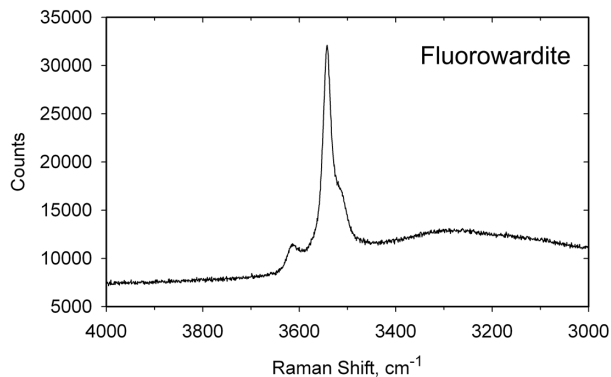


FIGURE 7. Raman spectrum of fluorowardite in the OH region.

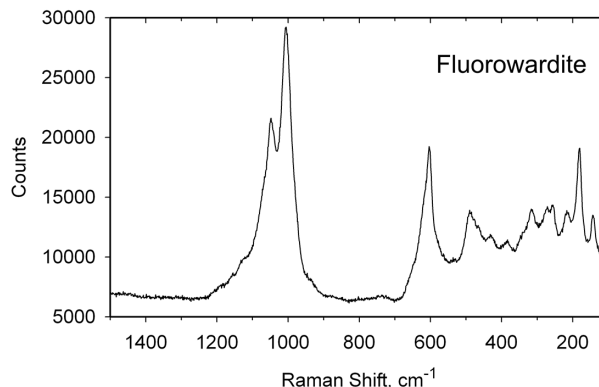


FIGURE 8. Raman spectrum of fluorowardite in the lower wavenumber region.

TABLE 1. Electron microprobe data for fluorowardite

Constituent	wt%	Min	Max	SD	Probe standard
Na ₂ O	6.27	5.14	7.11	0.67	Amelia albite
CaO	1.74	1.11	2.20	0.33	syn. anorthite
MgO	0.42	0.20	0.77	0.17	syn. forsterite
Al ₂ O ₃	35.21	34.47	36.01	0.51	syn. anorthite
Fe ₂ O ₃	0.72	0.41	1.07	0.20	syn. fayalite
P ₂ O ₅	32.49	31.40	33.61	0.68	Durango fluorapatite
As ₂ O ₅	0.64	0.00	1.56	0.56	syn. GaAs
F	6.76	6.34	7.23	0.33	fluorophlogopite
O=F	-2.85				
H ₂ O*	13.35				
Total	94.74				

* Calculated from the structure.

epoxy in a polished thin-section. After obtaining spectra from three of these crystals, one determined optically to be along a *c*-axis, it became obvious that, while not influencing the OH region, lines from the epoxy were contributing to the spectra in the lower wavenumber regions. Next, spectra were obtained from five unoriented crystals on one sample of fluorowardite coated botryoidal matrix and two crystals from another. The OH region of one of these crystals is shown in Figure 7.

For all 10 of the unoriented fluorowardite crystals measured, the ratio of the intensity of the high-energy peak (3614 cm⁻¹) to the low-energy peak (3452 cm⁻¹) is less than that of the lower ratio seen in the two wardite orientations. The average ratio in the unoriented crystals is less than one fourth the weighted average ratio seen in spectra from the oriented wardite crystal. This again is consistent with the view that the F is preferentially located on only one crystallographic site. The Raman spectrum of fluorowardite in the 1500–100 cm⁻¹ region (Fig. 8) is dominated by the phosphate bands at 1049, 1005, and 604 cm⁻¹. When Figure 8 is compared to Figure 6, it can be seen that there are many similarities, and that for fluorowardite there is a general broadening of several of the lines.

CHEMICAL COMPOSITION

Chemical analyses (8) were carried out using a JEOL 8200 electron microprobe in the Division of Geological and Planetary Sciences, California Institute of Technology (WDS mode, 15 keV, 1 nA, 10–20 μm beam diameter). Standards were run at 10 nA. Quantitative elemental microanalyses were processed

TABLE 2. Powder X-ray diffraction data for fluorowardite

<i>l</i> _{obs}	<i>d</i> _{obs}	<i>d</i> _{calc}	<i>l</i> _{calc}	<i>hkl</i>	<i>l</i> _{obs}	<i>d</i> _{obs}	<i>d</i> _{calc}	<i>l</i> _{calc}	<i>hkl</i>
9	6.639(15)	6.6116	12	101			1.7812	5	307
10	5.697(13)	5.6729	13	102	32	1.7628(2)	1.7614	30	400
19	5.000(7)	4.9821	31	110			1.7540	12	401
		4.8213	12	111			1.6979	4	403
100	4.766(2)	4.7827	44	004			1.6756	7	308
4	4.397(19)	4.4187	5	112			1.6661	5	326
5	3.977(6)	3.9571	10	104	29	1.6592(4)	1.6607	7	330
8	3.929(7)	3.9260	14	113			1.6545	4	331
2	3.517(14)	3.5229	3	200			1.6529	8	404
7	3.481(8)	3.4646	20	201			1.6506	3	413
4	3.450(14)	3.4502	2	114			1.6420	7	1·1·11
75	3.099(1)	3.1091	46	211	7	1.5968(6)	1.6000	4	405
		3.0836	66	203			1.5942	4	0·0·12
62	3.008(2)	3.0345	26	115	6	1.5597(9)	1.5896	5	327
		2.9928	75	212			1.5545	7	422
28	2.834(1)	2.8365	16	204	49	1.5228(2)	1.5295	20	423
		2.8249	35	213			1.5173	39	2·2·10
3	2.692(2)	2.6856	11	116	11	1.4574(2)	1.4964	3	424
		2.6312	10	214			1.4568	15	425
56	2.597(1)	2.5916	70	205			1.4405	4	1·0·13
		2.5480	14	107	17	1.4210(4)	1.4260	8	2·2·11
6	2.399(2)	2.3961	7	117			1.4182	6	408
		2.3640	4	206			1.4125	8	426
7	2.329(2)	2.3311	4	301	10	1.3906(7)	1.3941	5	502
		2.3203	7	223			1.3903	5	418
7	2.268(1)	2.2645	14	108			1.3818	4	510
9	2.166(1)	2.1700	5	312	9	1.3672(4)	1.3760	3	503
		2.1594	14	207			1.3670	4	3·2·10
28	2.109(1)	2.1081	31	304			1.3649	6	427
		2.1034	11	313	4	1.3320(4)	1.3579	3	2·0·13
8	2.078(2)	2.0876	4	225			1.3334	7	2·1·13
		2.0646	14	217	7	1.2978(3)	1.3190	3	3·0·12
13	2.022(2)	2.0350	7	109			1.2963	11	522
		2.0197	6	314	2	1.2663(7)	1.2679	2	516
		2.0016	6	305			1.2657	2	429
10	1.9644(6)	1.9630	16	226			1.2620	2	524
		1.9440	3	321			1.2525	3	507
20	1.9257(5)	1.9254	19	315	12	1.2465(3)	1.2470	2	3·0·13
		1.9146	6	322			1.2455	6	440
		1.9049	4	218	5	1.2135(4)	1.2429	5	441
6	1.8691(7)	1.8684	11	323			1.2140	7	438
		1.8410	3	227	7	1.2010(3)	1.2011	4	3·3·11
		1.8263	2	316			1.1992	7	2·0·15
7	1.8253(9)	1.8200	8	209					

Notes: Calculated lines with intensities less than 3 are not shown, unless they correspond to observed lines. Because the pattern was recorded using MoK α radiation, some significant calculated lines are contained in the shoulders of observed peaks.

TABLE 3. Data collection and structure refinement details for fluorowardite

Diffractionmeter	Rigaku R-Axis Rapid II
X-ray radiation/power	MoK α ($\lambda = 0.71075$ Å)/50 kV, 40 mA
Temperature	298(2) K
Structural formula	(Na _{0.96} Ca _{0.02})Al ₃ P _{1.86} O ₈ (OH) _{2.32} F _{1.68} (H ₂ O) ₂
Space group	P ₄ ,2,2
Unit-cell dimensions	$a = 7.077(2)$ Å $c = 19.227(3)$ Å
V	962.8(5) Å ³
Z	4
Density (for above formula)	2.738 g/cm ³
Absorption coefficient	0.865 mm ⁻¹
F(000)	791
Crystal size	60 × 50 × 35 μm
θ range	3.58 to 20.80°
Index ranges	-7 ≤ h ≤ 7, -7 ≤ k ≤ 7, -19 ≤ l ≤ 18
Reflections collected/unique	3412/498 (R _{int} = 0.086)
Reflections with F _o > 4σF	436
Completeness to θ = 20.80°	99.7%
Max. and min. transmission	0.97 and 0.95
Refinement method	Full-matrix least-squares on F ²
Parameters refined	104
GoF	1.060
Final R indices [F _o > 4σF]	R ₁ = 0.0315, wR ₂ = 0.0640
R indices (all data)	R ₁ = 0.0387, wR ₂ = 0.0660
Flack parameter	-0.4(5)
Largest diff. peak/hole	+0.25/-0.24 e/Å ³

Notes: R_{int} = Σ|F_o - F_o(mean)|/Σ|F_o|. GoF = S = {Σ[w(F_o² - F_c²)]/(n - p)}^{1/2}. R₁ = Σ||F_o - F_c||/Σ|F_o|. wR₂ = {Σ[w(F_o² - F_c²)]/Σ[w(F_o²)]}^{1/2}. w = 1/[σ²(F_o²) + (aP)² + bP] where a is 0.0283, b is 0, and P is [2F_c² + Max(F_o², 0)]/3.

with the CITZAF correction procedure. There was insufficient material for CHN analyses, so H₂O was calculated on the basis of Al + Fe = 3, charge balance and 14 total anions (O + F) pfu, as determined by the crystal-structure analysis (see below). The presence of H₂O and OH and the absence of CO₃ were further confirmed by FTIR spectroscopy (see above). Note that fluorowardite is very prone to electron beam damage (melting), which contributes to the low analytical total. We carefully monitored Na and F and confirmed that they remained constant during the analyses. We believe that sample melting mitigated charge build up at the electron penetration depth and hence eliminated any significant F or Na migration during the analyses. Analytical data are given in Table 1.

The empirical formula (based on 14 anions) is: (Na_{0.87}Ca_{0.13}Mg_{0.04}Σ_{1.04}(Al_{2.96}Fe_{0.04}Σ_{3.00}(P_{1.96}As_{0.03}Σ_{1.99}O_{8.12}(OH)_{2.32}F_{1.53}·2H₂O. The ideal formula is NaAl₃(PO₄)₂(OH)₂F₂·2H₂O, which requires Na₂O 7.71, Al₂O₃ 38.05, P₂O₅ 35.32, F 9.45, H₂O 13.45, O=F -3.98, total 100 wt%.

The Gladstone-Dale compatibility index 1 - (K_p/K_c) as

defined by Mandarino (1981) provides a measure of the consistency among the average index of refraction, calculated density, and chemical composition. For fluorowardite, the compatibility index is -0.002 based on the empirical formula, within the range of superior compatibility.

X-RAY CRYSTALLOGRAPHY AND STRUCTURE REFINEMENT

Both powder and single-crystal X-ray studies were carried out using a Rigaku R-Axis Rapid II curved imaging plate microdiffractometer, with monochromatized MoK α radiation. For the powder-diffraction study, a Gandolfi-like motion on the ϕ and ω axes was used to randomize the sample and observed d -spacings and intensities were derived by profile fitting using JADE 9.3 software. The powder data are presented in Table 2. Unit-cell parameters refined from the powder data using whole pattern fitting are: $a = 7.0458(13)$, $c = 19.131(4)$ Å, and $V = 949.7(3)$ Å³.

Even after considerable effort in selecting a fluorowardite crystal for structure data collection, the best crystal found was quite small (60 × 50 × 35 μm) and of marginal quality. Consequently, the data set was rather limited and much less than optimal relative to the number of parameters refined. The Rigaku CrystalClear software package was used for processing the structure data, including the application of an empirical multi-scan absorption correction using ABCOR (Higashi 2001). The SHELXL-97 software (Sheldrick 2008) was used for the refinement of the structure. The starting atom coordinates for the structure refinement were taken from the structure determination of wardite by Fanfani et al. (1970). Bond-valence considerations clearly indicate that the O5 and O7 sites in the wardite structure are the only possible sites for F. Refining both of these sites with joint occupancy by O and F showed the O7 site to be fully occupied by O and the O5 (F5) site to be mostly occupied by F. H-atom positions were located in difference Fourier maps and were constrained to H-O distances of 0.9(3) Å and an H-H distance for the H₂O of 1.45(3) Å. The isotropic displacement parameters (×1.2) were tied to those of the O atoms to which they are associated. The location of an H site related to O7 (OH7) is further corroboration that this site is OH rather than F. It should also be noted that the infrared and Raman spectroscopy (see above) also support the conclusion that F preferentially occupies one of these sites. In the final refinement, the occupancy of the F5 site refined to 0.84 F and

TABLE 4. Atom coordinates and displacement parameters (Å²) for fluorowardite

	x/a	y/b	z/c	U _{eq}	U ₁₁	U ₂₂	U ₃₃	U ₂₃	U ₁₃	U ₁₂
P ^a	0.1467(3)	0.3626(2)	0.34832(8)	0.0113(8)	0.0106(14)	0.0129(13)	0.0103(11)	-0.0012(9)	0.0008(8)	0.0008(8)
Al1	0.4038(3)	0.1014(3)	0.25947(9)	0.0153(6)	0.0162(13)	0.0147(13)	0.0150(11)	-0.0014(9)	0.0024(9)	0.0009(8)
Al2	0.0953(3)	0.0953(3)	0.0000	0.0158(8)	0.0152(11)	0.0152(11)	0.0172(16)	0.0005(10)	-0.0005(10)	-0.0018(14)
Na ^a	0.3851(4)	0.3851(4)	0.5000	0.0310(16)	0.027(2)	0.027(2)	0.038(3)	-0.0034(13)	0.0034(13)	0.008(2)
O1	0.0296(6)	0.4144(5)	0.3066(2)	0.0160(12)	0.011(3)	0.019(3)	0.018(3)	0.004(2)	-0.004(2)	0.002(2)
O2	0.3046(6)	0.5121(6)	0.33587(19)	0.0196(12)	0.017(3)	0.020(3)	0.022(3)	0.000(2)	0.001(2)	-0.006(2)
O3	0.2131(6)	0.1666(6)	0.3224(2)	0.0213(14)	0.019(3)	0.022(3)	0.023(3)	-0.001(2)	0.003(2)	0.001(2)
O4	0.1041(6)	0.3547(6)	0.4267(2)	0.0197(12)	0.014(3)	0.025(3)	0.020(2)	0.000(2)	0.000(2)	0.001(2)
F5 ^a	0.1263(5)	0.3470(5)	-0.03794(17)	0.0242(17)	0.024(3)	0.021(3)	0.027(2)	0.0033(19)	-0.0002(19)	0.0004(18)
OW6	0.1941(8)	0.0324(7)	0.1930(2)	0.0257(14)	0.028(4)	0.024(4)	0.025(3)	0.008(3)	-0.003(3)	0.005(3)
H6a	0.155(9)	0.104(6)	0.160(2)	0.031						
H6b	0.203(9)	-0.087(4)	0.180(3)	0.031						
OH7	0.4114(6)	0.3446(6)	0.2179(2)	0.0188(13)	0.021(3)	0.019(3)	0.017(3)	0.002(2)	0.001(2)	0.005(2)
H7	0.486(7)	0.327(9)	0.182(2)	0.023						

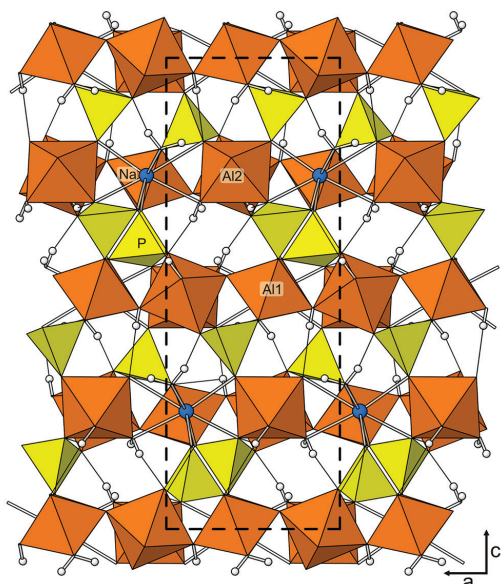
^a Refined site occupancies: P: 0.929(8); Na: 0.980(15) Na, 0.020(15) Ca; F5: 0.84(7) F, 0.16(7) O.

TABLE 5. Selected bond distances (Å) and angles (°) in fluorowardite

P-O1	1.528(5)	Al1-O3	1.871(4)	Al2-OH7 ^a	1.879(5)	Na-O4	2.446(5)
P-O4	1.539(4)	Al1-O1	1.878(5)	Al2-O2 ^a	1.891(4)	Na-O1 ^a	2.458(4)
P-O3	1.547(5)	Al1-F5	1.894(5)	Al2-F5 ^a	1.937(5)	Na-OW6 ^a	2.514(6)
P-O2	1.557(4)	Al1-OH7	1.898(5)	<Al-φ>	1.902	Na-O3 ^a	2.732(5)
<P-O>	1.543	Al1-O4	1.899(5)			<Na-O>	2.538
		Al1-OW6	2.018(5)				
		<Al-φ>	1.910				

Hydrogen bonds (D = donor, A = acceptor)

D-H	d(D-H)	d(H···A)	<DHA	d(D···A)	A	<HDH
OW6-H6a	0.86(3)	1.86(4)	161(6)	2.690(6)	O2	113(4)
OW6-H6b	0.88(3)	2.15(4)	145(5)	2.912(6)	F5	
OH7-H7	0.88(3)	2.47(3)	174(5)	3.354(6)	O3	

^a (×2).**FIGURE 9.** The structure of fluorowardite viewed along [010]. Hydrogen atoms are shown as spheres. Na-φ and O-H bonds are shown as sticks. Hydrogen bonds are shown as single lines. The outline of the unit cell is shown by thick dashed lines. (Color online.)

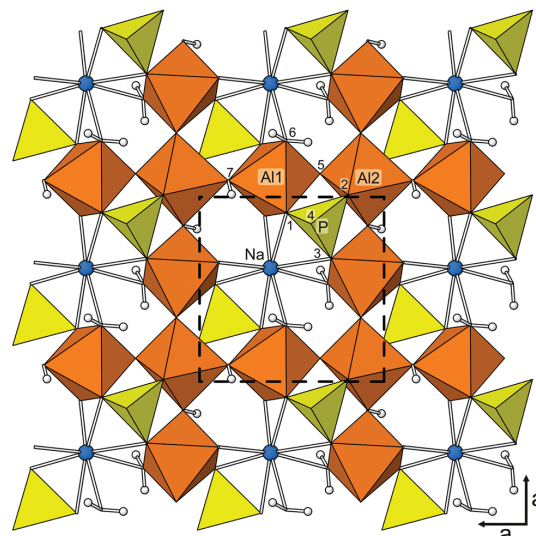
0.16 O, in reasonable agreement with the EMPA, which fits an occupancy of 0.77 F and 0.23 O for the site.

Details of data collection and structure refinement are provided in Table 3. Fractional coordinates and atom displacement parameters are provided in Table 4, selected interatomic distances in Table 5, and bond valences in Table 6. (CIF and supplemental table¹ available on deposit.)

TABLE 6. Bond-valence analysis for fluorowardite

	O1	O2	O3	O4	F5	OW6	OH7	Σ
P	1.23	1.14	1.17	1.19				4.73
Al1	0.53		0.54	0.50	0.41	0.36	0.50	2.84
Al2		0.51 ×2→			0.36 ×2→		0.53 ×2→	2.80
Na	0.17 ×2→		0.08 ×2→	0.18 ×2→		0.15 ×2→		1.16
H6a		0.21				0.79		1.00
H6b					0.09	0.91		1.00
H7			0.07				0.93	1.00
Σ	1.93	1.86	1.86	1.87	0.86	2.21	1.96	

Notes: Values are expressed in valence units. The bond strengths for the F5 site are based upon the refined site occupancy (0.84 F and 0.16 O). Multiplicity is indicated by ×→. P²⁺-O and Al-O bond strengths are from Brese and O'Keeffe (1991). Al-F and Na-O bond strengths are from Brown and Altermatt (1985). Hydrogen-bond strengths are based on H···O bond lengths, from Brown and Altermatt (1985); however, because X-ray diffraction locates the centroid of the electron density rather than the position of the nucleus, the determined H atom positions are too close to the donor atom by about 0.1 Å. Consequently, the H···O/F bond lengths listed in Table 4 have been reduced by 0.1 Å for determination of the hydrogen bond strengths.

**FIGURE 10.** One layer in structure of fluorowardite viewed along [001]. Anion sites (O1, O2, O3, O4, F5, OW6, and OH7) are numbered. The outline of the unit cell is shown by thick dashed lines. (Color online.)**DESCRIPTION OF THE STRUCTURE**

The structure (Figs. 9 and 10) contains layers parallel to {001} consisting of Alφ₆ (φ = F, O, OH, or H₂O) octahedra, PO₄ tetrahedra, and NaO₆(H₂O)₂ polyhedra. The two independent Alφ₆ octahedra link by corner-sharing to form a square array, in which each Al2 octahedron shares four corners with Al1 octahedra and each Al1 octahedron shares two *trans* corners with Al2 octahedra. Each PO₄ tetrahedron shares corners with three adjacent octahedra in the same square array and a fourth corner with an octahedron in the next layer. The Na atoms reside in the “cavities” in the square array, forming bonds only to O atoms in the same layer. The only linkages between the layers are the aforementioned tetrahedron-octahedron shared corner and hydrogen bonds.

The F5 and OH7 sites are the shared vertices between the Al octahedra. The Al1 octahedron includes one F5 and one OH7 atom, which are *trans* to one another. The Al2 octahedron

¹ Deposit item AM-14-403, Table and CIF. Deposit items are stored on the MSA web site and available via the *American Mineralogist* Table of Contents. Find the article in the table of contents at GSW (ammin.geoscienceworld.org) or MSA (www.minsocam.org), and then click on the deposit link.

includes two *cis* F5 and two *cis* OH7 atoms arranged around the girdle of the octahedron. Considering the clear preference of F for the F5 site, it is particularly intriguing that, discounting hydrogen bonding, there is no clear-cut topological difference between the F5 and OH7 sites.

The H atom of the OH7 group in fluorowardite is positioned to participate in a very weak hydrogen bond to O3 at an O–O distance of 3.354 Å and, although the H positions for wardite have not been determined, the OH7–O3 distance of 3.38 Å in the wardite structure is also likely to correspond to a weak hydrogen bond. The hydrogen bond acceptor for the OH5 group in wardite is not clear. The nearest possible acceptor is OW6, at a distance of 2.83 Å, but OW6 is already significantly bond-valence oversaturated (2.09 v.u. based on bond distances reported by Fanfani et al. 1970) and is almost certainly a hydrogen bond donor to OH5. The other possibility is O1, at a distance of 3.34 Å, but it is also bond-valence oversaturated (2.05 v.u.). The hydrogen bonding in the structures of fluorowardite and wardite mainly involves the H atoms of the OW6 group. In both structures, the OW6 group donates one hydrogen bond to O2 (at O–O distances of 2.690 Å in fluorowardite and 2.64 Å in wardite) and one hydrogen bond to F5/OH5 (at O–F distances of 2.912 Å in fluorowardite and 2.83 Å in wardite). There is no possibility for even a weak hydrogen bond from OW6 to OH7 in either structure.

It is noteworthy that the F5 site in the fluorowardite structure is significantly bond-valence undersaturated (0.86 v.u.), and that it would be much more undersaturated were it not for the hydrogen bond received from the OW6 group. If F occupied the OH7 site, then that site would be even more undersaturated than the F5 site, because it would receive no bond-strength contribution from a hydrogen bond. Furthermore, if the OH7 site were occupied by F, it could not donate a hydrogen bond to O3, leaving O3 highly bond-valence undersaturated (1.79 v.u.). Considering the foregoing, it is clear that the hydrogen bonding in fluorowardite contributes significantly to the bond-valence balance and, hence, the stability of its structure, and it can be reasoned that it probably plays a significant role in the preference of F for the F5 site.

IMPLICATIONS

In the 117 years since wardite was first described, it has been reported to occur at dozens of localities, sometimes in association with F-bearing phosphates, such as fluorapatite, morinite, and fluellite; however, until now, the F-analog of wardite has never been reported, and we are unaware of any previous reports, published or unpublished, of F-bearing wardite. Fluorowardite is the fifth new mineral described from the

Silver Coin mine and all five of these species (the others being iangreyite, krásnoite, meurigite-Na, and zinclipscobite) occur in an unusual highly F-rich phosphate assemblage. While it is likely that fluorowardite can form only in environments highly enriched in F, it also seems likely that analyses of wardites occurring in only moderately F-rich environments will show them to contain some F.

ACKNOWLEDGMENTS

Reviewers Stuart Mills and Frédéric Hatert and Editor Keith Putirka are thanked for their constructive comments on the manuscript. Work at the California Institute of Technology was supported by grants from the Northern California Mineralogical Association and the National Science Foundation (EAR-0947956). The remainder of this study was funded by the John Jago Trelawney Endowment to the Mineral Sciences Department of the Natural History Museum of Los Angeles County.

REFERENCES CITED

- Breiter, D.K., Belz, H.-H., Hajba, L., Komlosi, V., Mink, J., Brehm, G., Colognesi, D., Parker, S.F., and Schwab, R.G. (2004) Combined vibrational spectra of natural wardite. *Journal of Molecular Structure*, 706, 95–99.
- Brese, N.E., and O'Keeffe, M. (1991) Bond-valence parameters for solids. *Acta Crystallographica*, B47, 192–197.
- Brown, I.D., and Altermatt, D. (1985) Bond-valence parameters from a systematic analysis of the inorganic crystal structure database. *Acta Crystallographica*, B41, 244–247.
- Chukanov, N.V., Pekov, I.V., Möckel, S., Zadov, A.E., and V.T. Dubinchuk. (2006) Zinclipscobite $ZnFe_2^{3+}(PO_4)_2(OH)_2$ —a new mineral. *Proceedings of the Russian Mineralogical Society*, 135, 13–18.
- Davison, J.M. (1896) Wardite: a new hydrous basic phosphate of alumina. *American Journal of Science*, 2, 154–155.
- Fanfani, L., Nunzi, A., and Zanazzi, P.F. (1970) The crystal structure of wardite. *Mineralogical Magazine*, 37, 598–605.
- Frost, R.L., and Xi, Y.F. (2012) A vibrational spectroscopic study of the phosphate mineral wardite $NaAl_3(PO_4)_2(OH)_4 \cdot 2H_2O$. *Spectrochimica Acta Part A: Molecular and Biomolecular Spectroscopy*, 93, 155–163.
- Higashi, T. (2001) ABSCOR. Rigaku Corporation, Tokyo, Japan.
- Kampf, A.R., Adams, P.M., Kolitsch, U., and Steele, I.M. (2009) Meurigite-Na, a new species, and the relationship between phosphofibrite and meurigite. *American Mineralogist*, 94, 720–727.
- Mandarino, J.A. (1981) The Gladstone-Dale relationship: Part IV. The compatibility concept and its application. *Canadian Mineralogist*, 19, 441–450.
- Mills, S.J., Kampf, A.R., Sejkora, J., Adams, P.M., Birch, W.D., and Plášil, J. (2011) Iangreyite: a new secondary phosphate mineral closely related to perhamite. *Mineralogical Magazine*, 75, 329–338.
- Mills, S.J., Sejkora, J., Kampf, A.R., Grey, I.E., Bastow, T.J., Ball, N.A., Adams, P.M., Raudsepp, M., and Cooper, M.A. (2012) Krásnoite, the fluorophosphate analogue of perhamite, from the Huber open pit, Czech Republic and the Silver Coin mine, Nevada. *Mineralogical Magazine*, 76, 625–634.
- Sheldrick, G.M. (2008) A short history of SHELX. *Acta Crystallographica*, A64, 112–122.
- Thomssen, D., and Wise, W.S. (2004) Special list: Silver Coin Mine, Iron Point district, Edna Mountains, Humboldt Co., Nevada, U.S.A. *International Micromounter's Journal*, 13, 7–8.

MANUSCRIPT RECEIVED JULY 9, 2013

MANUSCRIPT ACCEPTED OCTOBER 7, 2013

MANUSCRIPT HANDLED BY G. DIEGO GATTA